

SHORT COMMUNICATION

Mallard landing behavior on water follows a $\dot{\tau}$ -constant braking strategy

John G. Whitehead^{1,*}, Terrell Worrell² and John J. Socha²

ABSTRACT

Many flying animals use optic flow to control their flight. During landing maneuvers, pigeons, hummingbirds, bats, *Draco* lizards and bees use the $\dot{\tau}$ -constant braking strategy. This strategy regulates the approach by keeping the ratio of distance to an object and the rate of change of that distance constant. In keeping this ratio, $\dot{\tau}$, constant, a variety of deceleration profiles can lead to different collision avoidance behaviors. The landing behaviors listed above all qualify as controlled collisions, where the animal is decelerating into the object. We examined whether the same regulatory strategy is employed by mallards when landing on water. Video of mallard landing behavior was recorded at a local pond and digitized. Kinematic and τ parameters were calculated for each landing ($N=177$). The Pearson correlation coefficient for τ with respect to time to land was 0.99 ± 0.02 , indicating mallards employ a controlled-collision strategy. This result implies regulation by the birds to fix $\dot{\tau}$ as constant while landing (on average, 0.90 ± 0.13). In comparison with other active flyers, mallards use a higher value of $\dot{\tau}$ when landing (0.775 ± 0.109 , 0.710 ± 0.132 and 0.702 ± 0.052 for pigeons, hummingbirds and bats, respectively). This higher $\dot{\tau}$ may reflect physical differences in substrate from solid to liquid. The higher compliance of water in comparison to a solid substrate may reduce impact forces that could be injurious on a solid substrate, thereby enabling mallards to approach faster and expend less energy for costly, slow flight.

KEY WORDS: Controlled collision, *Anas platyrhynchos*, Tau theory, Optic flow, Kinematics

INTRODUCTION

A primary benefit of flight is the speed at which an organism can traverse its environment. However, transitions from and to stationary positions, takeoff or landing, can be biomechanically challenging (Bonser and Rayner, 1996; Provini et al., 2014). To take off, an organism must generate enough lift to exceed the force of gravity to allow for altitude gain. To land, an organism must generate forces to decelerate, but also regulate that deceleration in relation to the time to contact to avoid an injurious collision. One solution to regulating self-movement and object avoidance is based in optic flow (Serres and Ruffier, 2017). Optic flow, the rate of change at which objects and patterns move on the retina, is proposed

as a key component of vision used to regulate behaviors such as object collision avoidance and pursuit, but also landing (Gibson, 1958; Koenderink, 1986). Proposed originally by Gibson (1958), optic flow has become foundational to our understanding of how flight is regulated in a wide variety of taxa (Warren, 2006), including both vertebrates (birds; Bhagavatula et al., 2011; Dakin et al., 2016; Vo et al., 2016) and invertebrates (insects; Baird et al., 2013; Chakravarthi et al., 2018; Linander et al., 2015; Srinivasan et al., 1996; Taylor and Krapp, 2007; Wang et al., 2017). Yet, while optic flow explains how a subject's movement and position relative to their surroundings can be tracked, it does not explain how an organism regulates the information to navigate its environment.

One proposed theory for regulating optic flow concerns the parameter tau (τ) (Lee, 1976). Tau theory proposes that collision behavior can be regulated by controlling the ratio of the distance to the object of collision and the rate of change of that distance (Lee, 1976; Lee et al., 2009):

$$\tau = x/\dot{x}, \quad (1)$$

where x is the distance to the object and \dot{x} is the rate of change of that distance (Lee, 1976; Lee et al., 2009). Lee and colleagues hypothesized that the simplest way to regulate τ is to keep its rate of change ($\dot{\tau}$) constant, termed the $\dot{\tau}$ -constant braking strategy (Lee, 1976; Lee et al., 2009):

$$\dot{\tau} = C. \quad (2)$$


The value at which $\dot{\tau}$ is held constant corresponds to different patterns of deceleration throughout the approach (Lee et al., 2009), providing a mechanism to categorize collision strategies. Behaviors with a $\dot{\tau}$ of 0.5 or less barely reach the substrate or come up short, a collision-avoidance behavior (Lee, 1976). If $\dot{\tau}$ is greater than 0.5 and less than 1, collision will occur, but braking increases before impact, a controlled collision (Lee, 1976). Lastly, if $\dot{\tau}$ is greater than 1, the subject will accelerate into the substrate, an uncontrolled collision (Lee, 1976). Evidence of a $\dot{\tau}$ -constant strategy has been found in hummingbirds approaching a feeder (Lee et al., 1991), pigeons landing on a perch (Lee et al., 1993), gliding lizards landing on a tree (Khandelwal and Hedrick, 2020) and bees landing on a disc (Baird et al., 2013). With values of $\dot{\tau}$ in the range 0.7–0.8, these behaviors are controlled collisions (Lee, 1976), reflecting an approach strategy where the subject increasingly decelerates up to the point of contact.

However, one feature of landing on a trunk or perch is that the target can be relatively small, requiring precise control (Baird et al., 2013). If landing occurs on a larger surface such as a body of water, such precision in landing may not be required. In addition to the potentially lower requirement for spatial precision, water has different physical properties than do solid substrates. The compliance of a substrate is known to influence gait (McMahon, 1985); goats, for example, actively adjust limb stiffness to

¹Department of Biological Sciences, Virginia Tech, Blacksburg, VA 24060, USA.

²Department of Biomedical Engineering and Mechanics, Virginia Tech, Blacksburg, VA 24060, USA.

*Author for correspondence (whijo23@vt.edu)

 J.G.W., 0000-0002-6300-280X

compensate for compliance changes (Clites et al., 2019). Many birds that land on water impact the water and then continue translating on the surface (known as ‘skimming’), effectively diffusing the change in linear momentum of landing over a greater time and distance. Thus, landing on water may require different values of $\dot{\tau}$ or a different regime for how optic flow is regulated.

Here, we examined landings in mallards to explore the visual strategies of birds that land predominantly on water. Do water-landing birds use the same controlled-collision strategy employed by other animals that land on solid perches? Do lower precision requirements and a more physically compliant substrate enable mallards to use a greater range of $\dot{\tau}$ values? To address these questions, we used simultaneous recordings from multiple videocameras to determine the 3D kinematics of mallards landing on a pond, providing data on landing under natural conditions.

MATERIALS AND METHODS

Landing trajectories of mallard ducks (*Anas platyrhynchos* Linnaeus 1758) were recorded at a local pond in Blacksburg, VA, USA (37°13'10"N, 80°25'39.23"W), with approximate dimensions of 250×100 m. The pond is typically inhabited by a mixed flock of multiple species of waterfowl, but largely comprises a residential population of mallard ducks. This flock varied in size throughout the year. Point counts from four locations around the pond indicate the mean (\pm s.d.) number of mallards present is 56±24, with seasonal fluctuations above 100 driven by the presence of migratory individuals.

Camera setup and calibration

To analyze landings, we used video photogrammetry to obtain 3D coordinates of the landing trajectories.

Specifically, three videocameras (HERO4 Black, GoPro, Los Angeles, CA, USA) were placed along one segment of the shore to record water landings. The videocameras were set on tripods placed at a spacing of approximately 3–5 m between each camera, with the cameras approximately 30–50 cm above the ground and pointed towards the volume of interest (VOI), calibrated with a 0.94 m wand. The videocameras were set to maximize spatial resolution (‘wide view’ of 4 k and sampling rate of 30 frames s⁻¹). A remote control (WiFi Smart Remote, GoPro) was used to start recordings from all three cameras when a landing event was about to occur. Because this remote signal does not start the cameras simultaneously, we used a sound signal to synchronize the recordings *post hoc*. Specifically, radios (two-way radio UHF 400–470 MHz, BaoFeng Radio, Arlington, SD, USA) were attached to a leg of each tripod; a fourth radio was hand-held by the experimenter, who pulsed a tone 3 times, which was emitted simultaneously at the radio on each tripod (Jackson et al., 2016) at the beginning and end of each recording. Because each radio was the same distance to each camera, the sound was recorded on the audio track of the camera at the same time, reducing the error of the *post hoc* synchronization of any given recording (Jackson et al., 2016).

Spatial calibration of the volume of interest (VOI) was conducted once per recording. To calibrate the approximately 12×6×2 m VOI, the experimenter walked out into the water with a custom wand (length, 0.94 m). The wand was first held in a vertical position by one end such that gravity oriented the other end into the vertical axis. This position was used to determine the gravitational axis. Next, the experimenter slowly walked in a large horseshoe pattern from a position near the east shore, out to the mouth of the cove, then back along the west shore (closer to the cameras). While walking, the

experimenter always faced the cameras and slowly moved the wand in a random circular pattern down to the surface of the water then back up over the head, ‘painting’ the 3D space.

Recording

The experimenter sat approximately 8 m from the shore, providing a clear view of approaches made by ducks while remaining in range to trigger the cameras to record. No obvious landing behavior was required to trigger a recording. Instead, the cameras were triggered any time a mallard duck flew over any part of the cove, which served to maximize the number of recorded landings and eliminate bias in choice of locomotor events. To encourage landings, cracked corn was periodically sprinkled on the east shoreline and in the water.

Filming occurred intermittently for a total of 26 days across multiple seasons (December 2016 to March of 2017, and October 2018 to February 2019). Days of filming were typically separated by at least one day, because the ducks seemed to become satiated by the feed if recording occurred too frequently. Satiation appeared to lead to fewer landings, as the waterfowl were more likely to swim across the pond than to fly across it. Filming was frequently more successful in cold weather, with ducks appearing to be more aggressive about feed in such weather.

Recorded landings were only analyzed if the local wind speed of gusts during recording was below 5.4 m s⁻¹ on a handheld anemometer (WM-2 Ambient Weather handheld weather meter, Chandler, AZ, USA), classified as a gentle breeze on the Beaufort wind scale (Meteorological Office, 1961). This value was chosen based on a previous study, which found that landing waterfowl do not show a directional preference in relation to wind direction below windspeeds of 5.4 m s⁻¹ (Hart et al., 2013). From the 26 days of filming, only 10 days yielded suitable recordings based on this criterion; for those days, the highest recorded wind speed was 2.6 m s⁻¹, yielding 38 recordings containing 244 analyzable landings. Filming repeatedly at the same pond means there is a likelihood of resampling the same individual. An estimate of the probability of the same duck being filmed was found using:

$$P(S) = \binom{r}{S} \times \left(\frac{1}{n}\right)^S \times \left(\frac{n-1}{n}\right)^{r-S}, \quad (3)$$

where r is the number of independent filming events, defined as when a single cohesive recording is taken – landings were cut out for digitization and processing from these recordings *post hoc*. This value is lower than the total number of landings as frequently multiple ducks would land near simultaneously or in sequence. Therefore, the same duck could not be recorded landing twice within one of the 38 different filming events and we commonly would obtain multiple landings from a given filming event. S is the frequency of the event in question in the population – in this case, one unique individual. n is the population size. Using values of $r=38$, $S=1$ and $n=56$, the estimated probability of any individual being filmed twice is 35%. To estimate variance in this probability, we used one standard deviation of population size (± 24) in this formula to provide lower and upper bounds, resulting in a range of 30% to 37%.

Digitization of calibration and landings

Landing videos were processed and analyzed using Argus software (Jackson et al., 2016). First, videos were de-warped to remove the image distortion of the fish-eye lens of the camera, using the omnidirectional coefficients provided by Argus (Jackson et al., 2016; Scaramuzza et al., 2006). For each landing sequence, the three

videos were first synchronized based on the radio pulses in the audio tracks. Then, the VOI was calibrated through manual digitization of the wand moved through the landing area of the pond. The tips of the wand were digitized every 10 frames using the program Wand in Argus until wand points all along the breadth of the VOI were obtained. From those points, the direct linear transformation (DLT) coefficients were obtained (Jackson et al., 2016; Zhang, 2000). The maximum variance in wand length for a given digitization was ± 2.2 cm, representing the maximum uncertainty for a given digitization. From previous data, the length of the bill of a mallard is approximately 4 cm and the length of the body ranges from 40 to 66 cm (Johnsgard, 2010). Thus, the measurement uncertainty was smaller than the bill length and the body length, and considerably smaller than the length of the measured trajectories (range, 0.96–33.62 m).

To represent the position of the duck in its trajectory, we digitized a single point, the location where the neck meets the body. This point was chosen because it was the clearest landmark on the body visible throughout the wingbeat cycle. Digitization began as soon as this point was visible in the approach trajectory, and ended when the duck stopped in the water or upon observation of a tail-wag and wing rearrangement, which occurred consistently after landing. Within the sequence, the frame with the first impact on the water was identified for designation as time zero. The program Clicker in Argus (Jackson et al., 2016) was used for all digitization, including landing trajectories and calibrations.

Using the digitized points and the DLT coefficients, the 3D coordinates of each landing trajectory were calculated in Argus (Jackson et al., 2016). In 27% of the sequences (65 landings), it was not possible to reliably digitize where the neck meets the body during impact, which resulted from the distance or orientation of the subject from the cameras or obstruction of the view by another duck. These landings were removed, yielding a total of 177 landing sequences in the final dataset. Within these landings, there were also some short sequences in which the point where the neck meets the body could not be digitized, frequently resulting from obstruction by the wing during downstroke, which created gaps in the trajectory coordinates. These gaps were interpolated using an unscented Kalman filter and then smoothed using a 2nd order Butterworth filter (Yu et al., 1999) (see Supplementary Materials and Methods for details). Instantaneous velocities for each trajectory were calculated using finite differences based on the resulting smoothed trajectories.

Analysis of kinematic data

Because the mallards landed naturally, the landing trajectories occurred at various locations scattered within the large region of interest (Fig. 1A). To compare the trajectories, we aligned them *post hoc* using a custom Python code. The trajectories were rotated into a single vertical plane and then translated so that the location of impact became the origin. Then, the tracked points were iteratively rotated in the x - y plane until they lined up with the initial vector. Temporally, the moment of initial impact was set as time zero. Lastly, because some recordings included level flight, we truncated each sequence to only include descent, identified from the vertical velocity data. Sequentially, a landing consisted of a descending aerial approach, impact with the water, and skimming until the mallard's velocity approached zero (Fig. 1B).

Once position data were filtered, the instantaneous velocity and acceleration at each time point were calculated. To accomplish this, the 2nd order central, forward and backward finite differences were calculated based on the corresponding coefficients. Forward

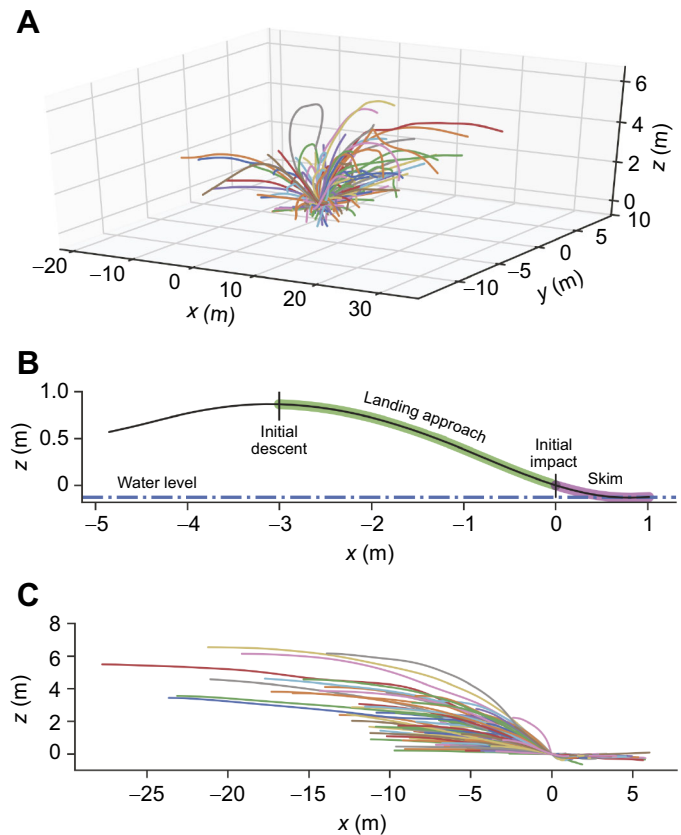


Fig. 1. Resulting tracking data from digitization and the transformations and selections done to make the landing data more comparable. (A) For all 177 landing trajectories, gaps were interpolated with a Kalman filter and trajectories were smoothed using a Butterworth filter; however, the resulting landings still approached and landed from a variety of directions, making comparisons difficult. Therefore, the trajectories were straightened into two dimensions, aligned with the initial point of impact for each duck at 0, and the beginning of the landing approach was set as the initial point of descent (B). This enabled each landing to be split into three distinct phases: the landing approach (green), the moment of initial impact, and the resulting skim after impact (purple). (C) The resulting trajectories after straightening, alignment to impact and selection of landing approach create a representation of the data that is easier to compare.

difference was used to calculate velocity and acceleration for the first time point in every trajectory,

$$v_0 = -1.5p_0 + p_1 - 0.5p_2, \quad (4)$$

$$a_0 = 2p_0 - 5p_1 + 4p_2 - p_3, \quad (5)$$

followed by a backward difference to calculate the velocity and acceleration at the end point in every trajectory:

$$v_{-1} = 1.5p_{-1} - 2p_{-2} + 0.5p_{-3}, \quad (6)$$

$$a_{-1} = 2p_{-1} - 5p_{-2} + 4p_{-3} - p_{-4}. \quad (7)$$

Lastly, gaps in velocity and acceleration were calculated by a central difference:

$$v_i = 0.5p_{i+1} - 0.5p_{i-1}, \quad (8)$$

$$a_i = p_{i+1} - 2p_i + p_{i-1}. \quad (9)$$

After gaps were interpolated and the resulting trajectories had been filtered, the data were translated such that the approach of all landings was from the same direction and the individual points were

rotated in line with the initial approach direction, effectively turning a 3D trajectory into 2D trajectory. To accomplish this transformation, first the initial approach angle in the x - y plane, μ , was found as:

$$\mu = -\tan^{-1}(p_x/p_y). \quad (10)$$

Next, a matrix was used to rotate the coordinates about this angle:

$$M_R = \begin{bmatrix} \cos \mu & -\sin \mu & 0 \\ \sin \mu & \cos \mu & 0 \\ 0 & 0 & 1 \end{bmatrix}. \quad (11)$$

With this rotation matrix, the position of a trajectory was iteratively rotated for each sequential point. The dot product of the change in position between two time points, Δp_i , and the rotation matrix gives the displacement from the previous position, p_{i-1} . The calculated displacement was then added to the previous position to find the coordinates for the straightened trajectory, p_s :

$$p_s = (M_R \cdot \Delta p_i) + p_{i-1}. \quad (12)$$

Once position was rotated, the non-position variables, velocity and acceleration, were rotated in a similar fashion. Both velocity and acceleration were rotated along the yaw axis of the 3D data; therefore, the yaw angle, θ , was calculated based on the velocity in the x - y plane:

$$\theta = -\tan^{-1}(v_x/v_y), \quad (13)$$

which required a rotation matrix of its own:

$$\theta_R = \begin{bmatrix} \cos \theta & \sin \theta & 0 \\ -\sin \theta & \cos \theta & 0 \\ 0 & 0 & 1 \end{bmatrix}, \quad (14)$$

with which both velocity and acceleration can be iteratively rotated using the dot product:

$$v_s = \theta_R \cdot v_i, \quad (15)$$

$$a_s = \theta_R \cdot a_i. \quad (16)$$

Plots for vertical velocity and horizontal velocity, as well as the resulting magnitude of velocity throughout the flight trajectories, are given in Fig. S1.

Extracting kinematic parameters

From each landing trajectory, the following kinematic parameters were extracted: horizontal impact velocity, vertical impact velocity, impact speed, impact angle, mean approach angle and distance after impact. Impact speed is the magnitude of the horizontal and vertical velocity vectors at impact:

$$|\vec{v}_{\text{imp}}| = \sqrt{v_{xy}^2 + v_z^2}. \quad (17)$$

Instantaneous trajectory angle throughout the landing trajectories was defined as the angle of the resultant velocity vector from the velocity vectors in the x and z direction. Impact angle is the trajectory angle calculated from velocity at impact:

$$\gamma = -\tan^{-1}(v_z/v_{xy}). \quad (18)$$

Mean approach angle is the mean of all instantaneous trajectory angles between the point of initial descent to impact. The point of initial descent was defined as the first moment in a trajectory when $v_z < 0$. Distance after impact was calculated by summing the

distances traveled between each time point during the skim:

$$d = \sum_{t_{\text{end}}}^{t_{\text{imp}}} \sqrt{(xy_t - xy_{t+1})^2 + (z_t - z_{t+1})^2}. \quad (19)$$

The skimming phase was defined as the point of impact until the mallard performed a tail waggle and/or wing rearrangement. The tail waggle and wing rearrangement were used as a reference to determine the end of skimming after a landing because mallards frequently did not come to a stop at the end of a skim. Instead, mallards would begin moving by paddling, which is a behavior we wanted to exclude. Therefore, these behaviors were identified as repeated behaviors the ducks would do regardless of whether they came to a complete stop after impacting the water.

Calculating τ and $\dot{\tau}$

The variable τ represents the distance to the object or collision divided by the rate of change of that distance. Therefore, τ was calculated as the horizontal distance to the point of impact divided by the instantaneous horizontal velocity for each moment in time:

$$\tau = \frac{|p_{xy}|}{v_{xy}}. \quad (20)$$

To calculate $\dot{\tau}$, we followed the methods of Lee et al. (1993), using the slope of the best-fit linear regression of τ versus time for each landing. The slope was calculated from a Pearson linear regression as a Pearson linear coefficient for the τ of each individual trajectory, using the SciPy.Stats package in Python. For this study, we chose to use the horizontal velocity rather than the total velocity to assess τ , in order to directly compare values with the pigeon landing behavior examined previously (Lee et al., 1993). Based on the resulting τ , with respect to time, the Pearson correlation coefficient was calculated for each individual trajectory to test whether mallards were using a $\dot{\tau}$ -constant braking landing. In addition, the rate of change of τ for a given landing, $\dot{\tau}$, was calculated based on the slope of the line of best fit for each trajectory, as in Lee et al. (1993).

RESULTS AND DISCUSSION

3D data from 177 trajectories revealed that during the landing approach, ducks descend at relatively shallow angles (8.6 ± 6.3 deg from the horizontal; mean \pm s.d.), with the trajectory becoming more steep (14.8 ± 10.0 deg) prior to impact. With an impact speed of 5.0 ± 1.4 m s⁻¹, the ducks skimmed 2.2 ± 1.3 m, representing approximately 3 body lengths of travel (measured from tip of bill to base of tail, as in Johnsgard, 2010).

The Pearson correlation coefficient of τ for all landings was 0.99 ± 0.01 , with a $\dot{\tau}$ of 0.90 ± 0.13 (Fig. 2A). The distribution of $\dot{\tau}$ obtained indicates there is a wide variety of behaviors performed by the mallards (Fig. 3A). In a subset of landings (18%; $n=32$), $\dot{\tau}$ was greater than 1 (Fig. 3B), suggesting some individuals accelerated as they impacted the water. To test whether these values represent a distinct behavior from the other landings, a non-parametric Mann-Whitney U -test for independence in impact speed, impact angle, approach angle or distance after impact was conducted. For landings with $\dot{\tau}$ greater than 1, mean (\pm s.d.) $\dot{\tau}$ was 1.09 ± 0.10 ; for those less than 1 it was 0.86 ± 0.09 . Only approach angle was statistically different from that of other landings: 6.9 ± 7.5 deg, slightly lower than that for landings with a $\dot{\tau}$ below 1, 8.9 ± 6.0 deg ($P < 0.01$).

The high level of linear correlation shown by the Pearson correlation coefficient (0.99 ± 0.01) between τ and time to impact strongly supports the hypothesis that mallards use a $\dot{\tau}$ -constant

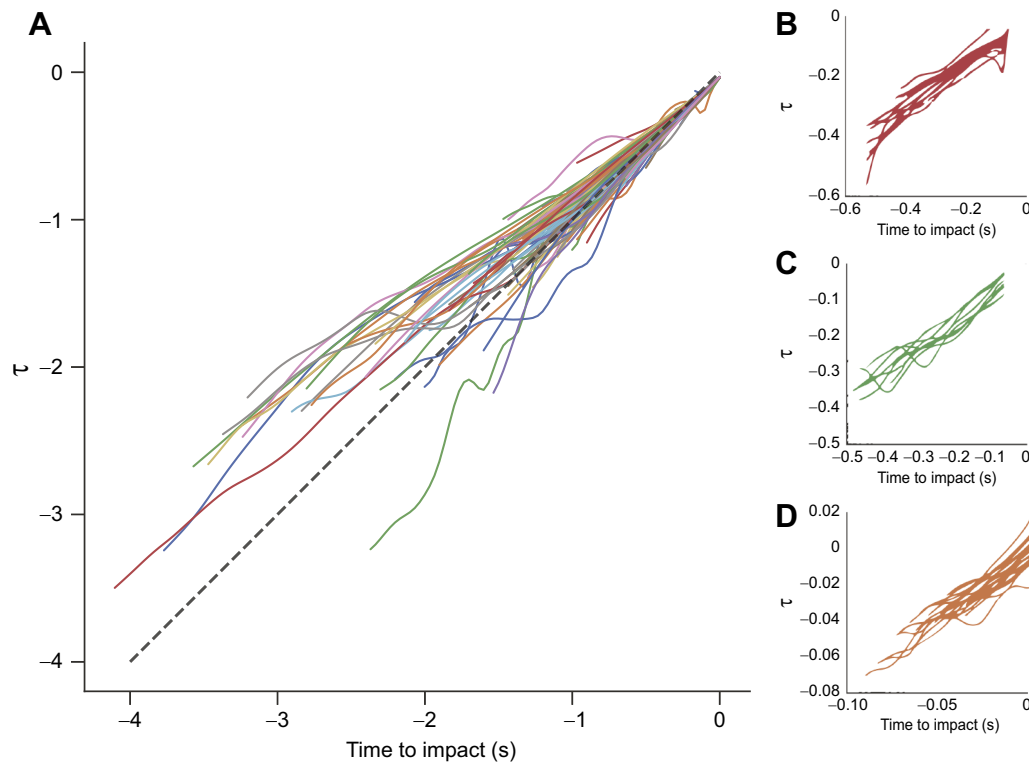


Fig. 2. τ values for landing trajectories. (A) The τ for each mallards' landing approach with respect to time until impact. Each line represents one landing ($N=177$) and the τ that individual has at each point in time based on the distance to initial impact and horizontal velocity at that moment. Recorded landings are different lengths, but there is a general and highly significant trend of linearity for τ in the landing trajectories. For all the landings, the mean Pearson linear coefficient was 0.99 ± 0.02 . (B) Values of τ found for pigeons (*Columbia livia*) landing on a perch (Lee et al., 1993). (C) τ found for big brown bats (*Eptesicus fuscus*) landing on a hand (Lee et al., 1995). (D) τ found for hummingbirds (*Colibri corsucans*) approaching a feeding tube (Lee et al., 1991). All of these studies demonstrate a linear behavior of τ in support of the utilization of a $\dot{\tau}$ -constant braking strategy.

braking strategy when landing on water. The mean value of $\dot{\tau}$, 0.90, is greater than 0.5 and less than 1, suggesting mallards employ a controlled-collision strategy (Lee, 1976). However, the standard deviation of $\dot{\tau}$ (± 0.13) in these landings includes 1, and the τ values tend to converge towards a slope of 1 (Fig. 2A; Fig. S2). This variance may indicate different styles of landing or an inclination to regulate τ to maintain a constant velocity right before

impact ($\dot{\tau}=1$). A one-tailed Wilcoxon signed-rank test indicates that the median value is likely to be below 1 ($P < 0.001$), which supports the τ maintenance hypothesis. Alternatively, some variation observed in $\dot{\tau}$ may result from the inclusion of descending flight where the bird is not actively regulating velocity for landing. Further study is needed to more carefully parse what are preparatory flight maneuvers and what is carefully regulated landing behavior.

A subset of landings exhibited a $\dot{\tau}$ greater than 1 and were associated with statistically shallower approach angles. Combined with less aerial deceleration, this behavior could result in greater skimming after impact. However, these shallower approaches did not lead to statistical differences in impact speed, impact angle or distance after impact, suggesting that impact and post-impact movement were not targets of performance. A direct comparison of landings on land versus water in mallards, under more controlled settings, is needed to analyze how higher $\dot{\tau}$ and possibly the use of $\dot{\tau}=1$ could be involved in landing behavior.

The use of a $\dot{\tau}$ -constant braking strategy by mallards landing on water is consistent with values observed experimentally in pigeons (*Columbia livia*; Lee et al., 1993), big brown bats (*Eptesicus fuscus*; Lee et al., 1995) and sparkling violet-ear hummingbirds (*Colibri corsucans*; Lee et al., 1991) (Fig. 2). However, the $\dot{\tau}$ values of mallards landing on water are greater than the mean values documented in these species' landing behaviors: pigeons 0.775 ± 0.109 (Lee et al., 1993), bats 0.702 ± 0.052 (Lee et al., 1995) and hummingbirds 0.710 ± 0.132 (Lee et al., 1991). This greater value of $\dot{\tau}$ for mallards also exceeds that seen for a gliding animal, *Draco* lizards, with a reported value of 0.84 ± 0.08

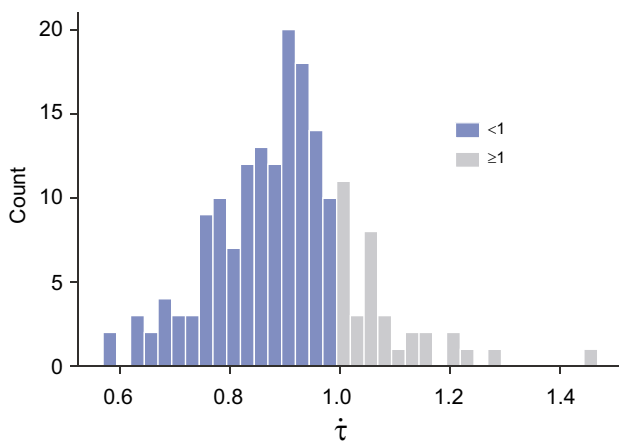


Fig. 3. Distribution of $\dot{\tau}$ values obtained for mallard landing trajectories. Frequency of $\dot{\tau}$ values for all landing trajectories of the mallards, with values equal to or greater than 1 indicated in grey. This value is of interest as it would imply those mallards are accelerating into the water as opposed to decelerating.

(Khandelwal and Hedrick, 2020). These arboreal gliders use a stall method of braking before impacting the trunk of a tree (Bahlman et al., 2013; Khandelwal and Hedrick, 2020).

Despite utilizing the same strategy with regard to τ , mallards landing on water brake less than birds landing on a perch (Lee et al., 1993). The faster approach may reflect physical differences enabled by impacting a liquid versus solid surface. First, landing on open water surfaces may require less precision than landing on a perch: a branch with a diameter of the order of centimeters is a much smaller target than an open water surface meters in length. Second, liquid water provides a more compliant surface than a fixed branch, enabling birds to impact the surface at higher speeds. Whether these two factors are mutually beneficial for water landing is unclear, as the reduced requisite precision and higher speeds may not coincide with reduced risk of failure or injury. For instance, failure or injury may result from a pitch-forward failure, which could occur if the feet contact first, producing a drag torque that rotates the center of mass of the body downward toward the water (effectively, a mallard face-plant). Regardless, approaching the water surface at higher speeds should entail lower energetic costs for water landing. Work on starlings, finches and doves (Bonser and Rayner, 1996; Provini et al., 2014) has shown that perch landing involves steeper approaches, and production of substantial aerodynamic forces that can be greater in landing than in take-off, which has subsequent implications for energetics.

Mallards landing on water utilize a similar τ -constant braking strategy to the landing behavior of pigeons and bats, and during feeder approach in hummingbirds. Yet, the τ values used by mallards appear higher, suggesting less deceleration. In addition, impact speeds are up to 4 times higher than those seen in pigeon perch landing. These differences in landing behavior compared with pigeons imply that mallards may be taking advantage of the inertial absorptive properties of landing on water to disperse higher-velocity landings with less deceleration. However, this study does not discern whether the differences in landing behavior between mallards and pigeons result from an active behavioral shift or a passive effect resulting from how optic flow is perceived. The difference in kinematics and τ values could reflect underlying mechanisms to reduce energy expenditure during landing, or be a side effect of a decreased ability to discern τ while landing on a more featureless water substrate, which could lower the accuracy of their perception of optic flow.

Acknowledgements

We thank Dr Ty Hedrick, Dr Brandon Jackson and Dr Dennis Evangelista for assistance in learning how to record, calibrate and synchronize cameras so animal behavior in the field can be tracked in three dimensions. In addition, we thank Isaac Yeaton and Talia Weiss for technical assistance in the development and implementation of data processing and analyses in Python. The results and discussion in this paper are reproduced in the PhD thesis of J.G.W. (Whitehead, 2020).

Competing interests

The authors declare no competing or financial interests.

Author contributions

Conceptualization: J.G.W., J.J.S.; Methodology: J.G.W., T.W., J.J.S.; Validation: J.G.W.; Formal analysis: J.G.W., T.W., J.J.S.; Investigation: J.G.W., T.W.; Resources: J.J.S.; Data curation: T.W.; Writing - original draft: J.G.W.; Writing - review & editing: T.W., J.J.S.; Visualization: J.G.W.; Supervision: J.J.S.; Project administration: J.G.W., J.J.S.; Funding acquisition: J.J.S.

Funding

This work was supported by a National Science Foundation Integrative Graduate Education and Research Traineeship (IGERT) (0966125).

Data availability

Data and scripts are available on GitHub: <https://github.com/whitejg/MallardLandingBehaviorFollowsTau>.

References

- Bahlman, J. W., Swartz, S. M., Riskin, D. K. and Breuer, K. S. (2013). Glide performance and aerodynamics of non-equilibrium glides in northern flying squirrels (*Glaucomys sabrinus*). *J. R. Soc. Interface* **10**, 20120794–20120794. doi:10.1098/rsif.2012.0794
- Baird, E., Boedeker, N., Ibbotson, M. R. and Srinivasan, M. V. (2013). A universal strategy for visually guided landing. *Proc. Natl. Acad. Sci. USA* **110**, 18686–18691. doi:10.1073/pnas.1314311110
- Bhagavatula, P. S., Claudianos, C., Ibbotson, M. R. and Srinivasan, M. V. (2011). Optic flow cues guide flight in birds. *Curr. Biol.* **21**, 1794–1799. doi:10.1016/j.cub.2011.09.009
- Bonser, R. H. C. and Rayner, J. M. V. (1996). Measuring leg thrust forces in the common starling. *J. Exp. Biol.* **199**, 435–439. doi:10.1242/jeb.199.2.435
- Chakravarthi, A., Rajus, S., Kelber, A., Dacke, M. and Baird, E. (2018). Differences in spatial resolution and contrast sensitivity of flight control in the honeybees *Apis cerana* and *Apis mellifera*. *J. Exp. Biol.* **221**, jeb184267. doi:10.1242/jeb.184267
- Clites, T. R., Arnold, A. S., Singh, N. M., Kline, E., Chen, H., Tugman, C., Billadeau, B., Biewener, A. A. and Herr, H. M. (2019). Goats decrease hindlimb stiffness when walking over compliant surfaces. *J. Exp. Biol.* **222**, jeb198325. doi:10.1242/jeb.198325
- Dakin, R., Fellows, T. K. and Altshuler, D. L. (2016). Visual guidance of forward flight in hummingbirds reveals control based on image features instead of pattern velocity. *Proc. Natl. Acad. Sci. USA* **113**, 8849–8854. doi:10.1073/pnas.1603221113
- Gibson, J. (1958). Visually controlled locomotion and visual orientation in animals. *Br. J. Psychol.* **49**, 182–194. doi:10.1111/j.2044-8295.1958.tb00656.x
- Hart, V., Malkemper, E. P., Kušta, T., Begall, S., Nováková, P., Hanzal, V., Pleskač, L., Ježek, M., Policht, R. and Husinec, V. (2013). Directional compass preference for landing in water birds. *Front. Zool.* **10**, 38. doi:10.1186/1742-9994-10-38
- Jackson, B. E., Evangelista, D. J., Ray, D. D. and Hedrick, T. L. (2016). 3D for the people: multi-camera motion capture in the field with consumer-grade cameras and open source software. *Biol. Open* **5**, 1334–1342. doi:10.1242/bio.018713
- Johnsgard, P. A. (2010). Tribe Anatini (Surface-Feeding Ducks). In *Ducks, Geese, and Swans of the World* (ed. U. of Nebraska), pp. 216–219. Lincoln.
- Khandelwal, P. C. and Hedrick, T. L. (2020). How biomechanics, path planning and sensing enable gliding flight in a natural environment. *Proc. Biol. Sci.* **287**, 20192888. doi:10.1098/rspb.2019.2888
- Koenderink, J. J. (1986). Optic flow. *Vision Res.* **26**, 161–179. doi:10.1016/0042-6989(86)90078-7
- Lee, D. N. (1976). A theory of visual control of braking based on information about time-to-collision. *Perception* **5**, 437–459. doi:10.1068/p050437
- Lee, D. N., Reddish, P. E. and Rand, D. T. (1991). Aerial docking by hummingbirds. *Naturwissenschaften* **78**, 526–527. doi:10.1007/BF01131406
- Lee, D. N., Davies, M. N. O., Green, P. R. and Van Der Weel, F. R. (1993). Visual control of velocity of approach by pigeons when landing. *J. Exp. Biol.* **180**, 82–104. doi:10.1242/jeb.180.1.85
- Lee, D. N., Simmons, J. A., Saillant, P. A. and Bouffard, F. (1995). Steering by echolocation: a paradigm of ecological acoustics. *J. Comp. Physiol. A* **176**, 347–354. doi:10.1007/BF00219060
- Lee, D. N., Bootsma, R. J., Frost, B. J., Regan, D. and Gray, R. (2009). Lee's 1976 paper. *Perception* **38**, 837–858. doi:10.1068/pmklee
- Linander, N., Dacke, M. and Baird, E. (2015). Bumblebees measure optic flow for position and speed control flexibly within the frontal visual field. *J. Exp. Biol.* **218**, 1051–1059. doi:10.1242/jeb.107409
- McMahon, T. A. (1985). The role of compliance in mammalian running gaits. *J. Exp. Biol.* **115**, 263–282. doi:10.1242/jeb.115.1.263
- Provini, P., Tobalske, B. W., Crandell, K. E. and Abourachid, A. (2014). Transition from wing to leg forces during landing in birds. *J. Exp. Biol.* **217**, 2659–2666. doi:10.1242/jeb.104588
- Scaramuzza, D., Martinelli, A. and Siegwart, R. (2006). A toolbox for easily calibrating omnidirectional cameras. In *IEEE International Conference on Intelligent Robots and Systems*, pp. 5695–5701. doi:10.1109/IROS.2006.282372
- Serres, J. R. and Ruffier, F. (2017). Optic flow-based collision-free strategies: From insects to robots. *Arthropod. Struct. Dev.* **46**, 703–717. doi:10.1016/j.asd.2017.06.003
- Srinivasan, M. V., Zhang, S. W., Lehrer, M. and Collett, T. S. (1996). Honeybee navigation en route to the goal: Visual flight control and odometry. *J. Exp. Biol.* **199**, 237–244. doi:10.1242/jeb.199.1.237
- Taylor, G. K. and Krapp, H. G. (2007). Sensory systems and flight stability: what do insects measure and why? *Adv. Insect Physiol.* **34**, 231–316. doi:10.1016/S0065-2806(07)34005-8
- Meteorological Office (1961). *The Meteorological Glossary* (3rd edn). London: H.M. Stationery Office.

- Vo, H. D., Schiffner, I. and Srinivasan, M. V.** (2016). Anticipatory manoeuvres in bird flight. *Sci. Rep.* **6**, 27591. doi:10.1038/srep27591
- Wang, H., Ando, N., Takahashi, H. and Kanzaki, R.** (2017). Visuomotor response to object expansion in free-flying bumble bees. *J. Insect Behav.*, **30**, 612-631. doi:10.1007/s10905-017-9645-x
- Warren, W. H., Jr** (2006). Visually controlled locomotion: 40 years later. *Ecol. Psychol.* **10**, 177-219. doi:10.1207/s15326969eco103&&4_3
- Whitehead, J. G.** (2020). An examination of the kinematics and behavior of mallards (*Anas platyrhynchos*) during water landings. PhD thesis, Virginia Tech.
- Yu, B., Gabriel, D., Noble, L. and An, K. N.** (1999). Estimate of the optimum cutoff frequency for the Butterworth low-pass digital filter. *J. Appl. Biomech.* **15**, 318-329. doi:10.1123/jab.15.3.318.
- Zhang, Z.** (2000). A flexible new technique for camera calibration. *IEEE Trans. Pattern Anal. Mach. Intell.* **22**, 1330-1334. doi:10.1109/34.888718